2024 6th International Conference on Reconfigurable Mechanisms and Robots (ReMAR)
June 24-27, 2024. Chicago, IL, USA

Robot Links: towards self-assembling truss robots*

Philippe Martin Wyder, Riyaan Bakhda, Meiqi Zhao, Quinn A. Booth, Simon Kang, Matthew Ethan Modi, Andrew Song, Jiahao Wu, Priya Patel, Robert T. Kasumi, David Yi, Nihar Niraj Garg, Siddharth Bhutoria, Evan H. Tong, Yuhang Hu, Omer Mustel, Donghan Kim and Hod Lipson

2024 6th International Conference on Reconfigurable Mechanisms and Robots (ReMAR) | 979-8-3503-9596-9/24/$31.00 ©2024 IEEE | DOI: 10.1109/REMAR61031.2024.10619984

***Abstract*—Today's monolithic robots act as closed systems that cannot absorb more material to keep operating after or recover from significant structural damage during their lifetime. Modular, reconfigurable robots offer a potential solution by discretizing the robot into replaceable and often identical modules that can self-assemble and self-rearrange. We introduce the Robot Link, a novel truss-robot module with magnetic connectors capable of self-assembly and re-forming broken connections. Each Robot Link can connect up to nine other Robot Links on either side and can thus form polygons and triangular lattice structures when combined with other Robot Links. Robot Links can crawl forward and backward, which allows them to move towards and connect to other links. We demonstrate a self-assembly sequence that shows individual Robot Links combining and transforming to form a tetrahedron, thereby demonstrating the first transformation of independent truss-robot modules that are limited to one-dimensional locomotion into a fully actuated, three-dimensionally maneuverable robot. Experiments revealed that Robot Link structures can reform broken connections, mimicking cells with reformable bonds. We demonstrate that three different robot topologies recover from separation after impact. This work contributes to developmental robotics by introducing a robotic substrate that enables robots to "grow" by integrating more material, self-improvement, and self-repair within their lifetime.**

I. Introduction

Despite significant progress in robotics research, today's robots are vulnerable to single points of failure and are limited in their ability to adapt their shape to specific tasks. To ensure a sustainable future for robots in our society, robots must become more versatile, more resilient, and be able to take care of themselves.

Inspired by nature, today's robots often come in the forms of arms or bipedal and quadruped robot designs [1], [2]. But unlike these machines, their biological counterparts sustain themselves, self-heal and grow by absorbing material from their environment and expelling waste: they operate as open systems[3]. We believe that for robots to become both resilient and self-sustaining, they need to be able to act as open systems during their lifespan.

We introduce a new kind of truss modular reconfiguring robot (MRR) that is capable of making itself bigger faster and more capable by integrating more material, and reform broken connections. These robots comprise one or more Robot Links (also referred to as *links*), the robot modules used for this research. We demonstrate the Robot Link robots' capacity to self-assemble and self-improve, and re-assemble after breaking apart. Further, we address the limitations and future work.

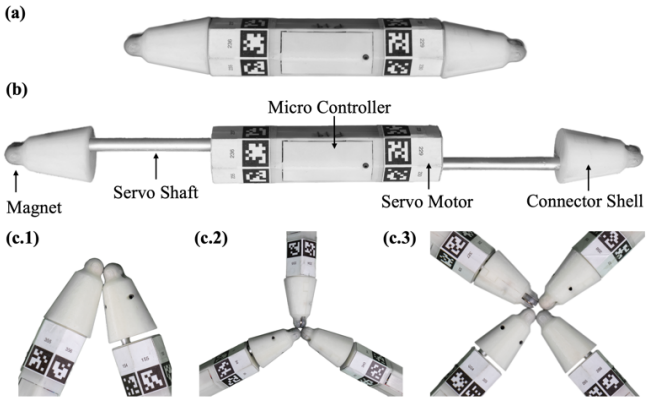


Figure 1. Robot Link. *(a) fully contracted Robot Link; (b) fully expanded Robot Link; (c.1-c.3) two, three, and four Robot Links connected at one point.*

II. Robot Links

The Robot Link is the building block of our homogenous, truss-style MRR system. Truss-style MRR form scaffold-like structures and have expanding and contracting modules[4]. Inspired by GEOMAG™ building sticks, Robot Links resemble hexagonal bars with magnetic connectors (see Fig. 1) that are 28cm long when contracted and 43cm long when expanded. The size of the Robot Link for this design was determined by the formfactor of the two 100mm stroke length Actuonix L12 linear servos that were chosen to maximize the expansion ratio of the link while minimizing the diameter of the link body. Both servos operate along the same axis but in opposite directions and thus enable the Robot Link to perform an inch-worm style crawl in one dimension (1D): forward and backward.

Links or *link* structures crawl by shifting the weight from the connector that needs to slide to the connector that needs to stay put—exploiting differential friction. The Robot Link contacts the ground on the ridge of the connector cones, while the body acts as a mass that can be transferred to increase friction at one contact point or another. We observed good crawling behavior on low-pile carpet and rubber surfaces. Robot Links crawl slowly on flat ground and are placed on a slope to speed up more complex experiments.

Robot Links are simple by design. They don't contain features that could be simulated in software: power sharing,

* Research supported in part by NSF AI Institute for Dynamical Systems #2112085, NSF NRI Award #1925157 and DARPA TRADES grant HR0011-17-2-0014.

All authors are with Columbia University, New York, NY 10027 USA (corresponding author philippe.wyder@columbia.edu).

Authorized licensed use limited to: University of Southern California. Downloaded on November 11,2025 at 22:32:37 UTC from IEEE Xplore. Restrictions apply.

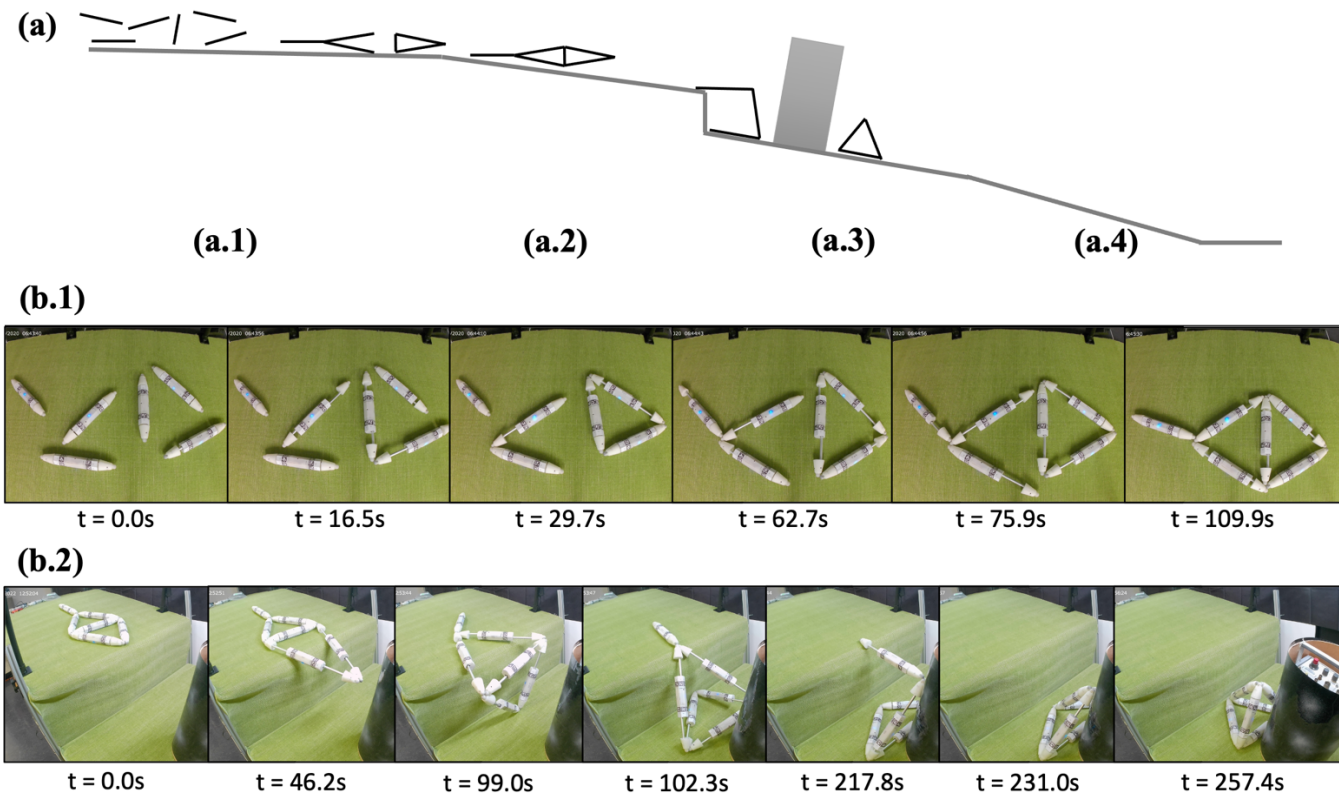


Figure 2. Formation of a tetrahedron from Robot Links. *(a) diagram showing the tetrahedron formation conceptually; (a.1-a.4) label the different stages of the experiment environment; (b.1) video frames showing the transformation from six individual Robot Links to a three-pointed star and a triangle that then combine to form a diamond-with-tail topology; (b.2) video frames shwoing the transformation from a diamond-with-tail to a tetrahedron.*

link-to-link communication, onboard sensors, etc. A *link* comprises only six different electrical components: servos, microcontroller, voltage regulator, resistors, WIFI antenna, and batteries. All body parts are 3D printed in PLA.

Earlier truss MRR burdened their connectors with communication and power-sharing channels and thus were incapable of self-assembly[5], [6]. Spinos et. al. and Park et al. introduced Variable Topology Truss (VTT), a heterogenous truss MRR comprising actuated bars and vertex spheres [7], [8]. Unlike these systems, Robot Links, due to their connector design, can not only self-reconfigure, but also self-assemble.

The free-form Robot Link connector can accept connections from a continuous range of angles excluding the space taken up by the connector cone itself. Thus, two *links* cannot connect with a connection angle of less than 0.37 radians measured along the central axis of the two links. Inside the connector is a positionally but not rotationally constrained half-inch N52 neodymium magnet sphere which rotates passively, ensuring equilibrium magnet alignment between connectors. We measured the in-line pull-away force required to separate two links at 13.7N. The magnet strength is sufficient for two links will snap together when they are an inch apart. The rotational freedom of the magnet sphere, allows multiple connectors to connect at one point without conflicts of polarity. Due to the connector geometry, Robot Link are unable to accept more than nine *link* connections at one point.

Free-form attachment is greedy and facilitates self-assembly in non-discretized environments and improves on discrete attachment styles for self-assembly[4]. For example, as was the case with Yim et. al's PolyBot and other early connector designs, the connector design used by Baca et. al and Roehr et. al. is limited to four possible attachment orientations between two connectors.[9], [10], [11], [12], [13] Most cube-shaped modular robot systems only allow for 24 possible attachment orientations, and thus require accurate alignment for successful connections.

Other free-form MRRs such as the FreeBot and FreeSN rely on fully ferromagnetic shells for connectivity and provide infinite attachment points on their entire body [14], [15]. Due to their spherical shape, FreeBot and FreeSN tend to produce dense structures—similar to the dense structures produced by cube-shaped MRRs. In contrast, Robot Links naturally form less-dense, truss-style structures, while still providing a continuous and thereby infinite number of attachment angles.

The Robot Links are programmed to execute commands received via WIFI from a Python server script: computation occurs offboard. On the server, each *link* operates as its own thread that handles communication and provides an interface for controller scripts to interact with by sending position commands to the servos. Unless stated otherwise, the experiment in this paper were conducted using a keyboard-based manual controller interface that can both expand and contract individual servos on individual *links* and execute pre-programmed motions. The pre-programmed motions include a single-link crawl, triangle crawl, diamond-with-tail (see frame t = 0 s in Fig. 2 b.2) crawl, and tetrahedron crawl and topple.

Authorized licensed use limited to: University of Southern California. Downloaded on November 11,2025 at 22:32:37 UTC from IEEE Xplore. Restrictions apply.

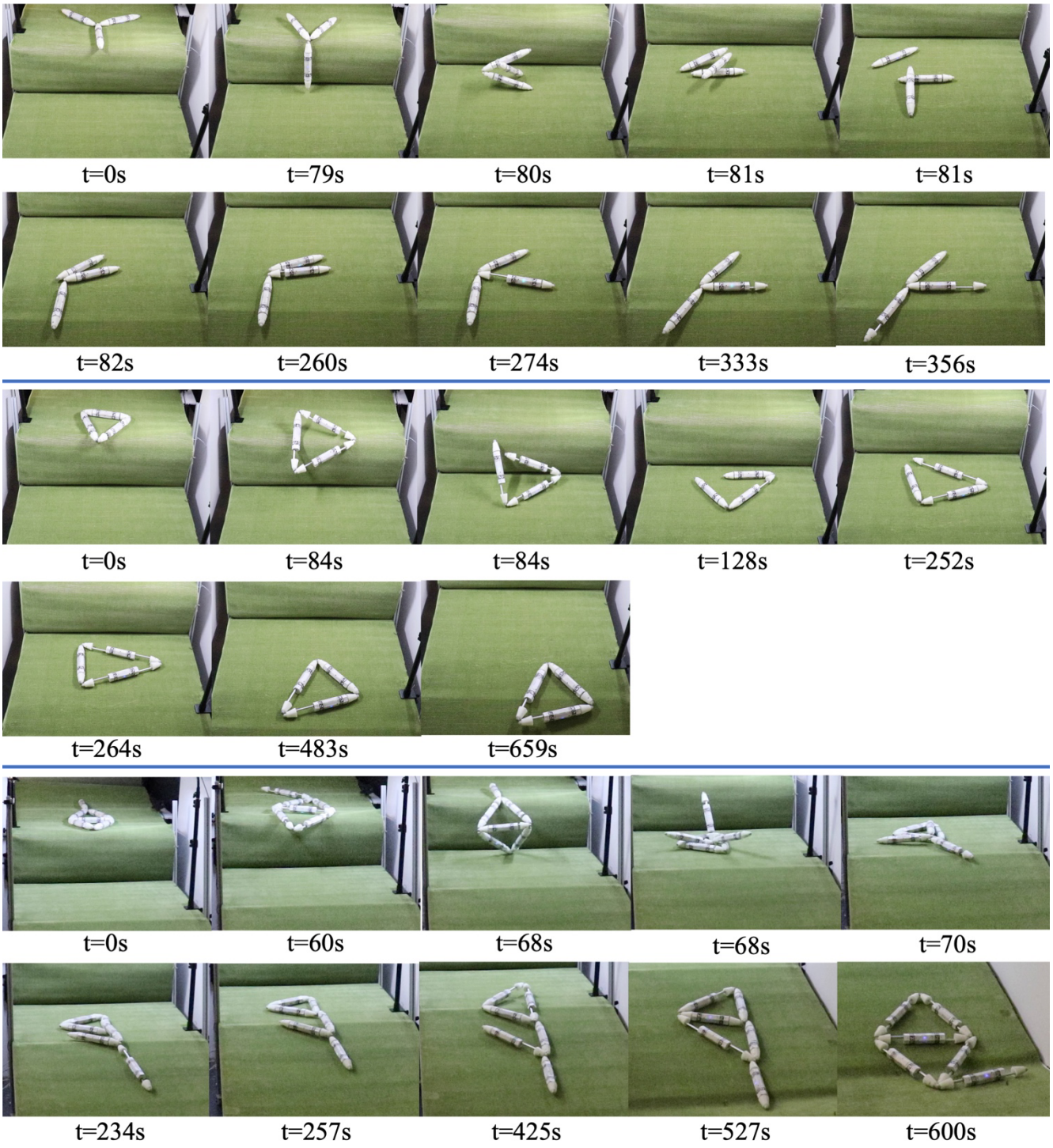


Figure 3. Robot Link topologies recovering from damage. *Video frame sequences showing a three-pointed star (top), a triangle (middle), and a diamond-with-tail (bottom) crawling off a ledge, breaking one, three, and two robot link connections respectively and then "heal" themselves.*

III. METHODS

First, we show how six individual *links* self-assemble to form a tetrahedron. Second, we show the Robot Link's ability to recover from separation due to impact for three robot topologies: triangle, three-pointed star, and diamond-with-tail. Finally, we show how a closed loop operated tetrahedron fetches a plastic sphere.

Planar and limited to movement in one dimension, Robot Links must exploit the environment topology or be assisted by other 3D robot structures to form three-dimensional structures. We used PyBullet to explore the Robot Link's dynamics in different environments to find a suitable terrain for forming a tetrahedron [16]. We then built a physical version of the simulated environment and used it for the *self-assembly* and *self-healing* experiment (see Fig. 2-a).

Authorized licensed use limited to: University of Southern California. Downloaded on November 11,2025 at 22:32:37 UTC from IEEE Xplore. Restrictions apply.

While the results in this paper are not simulation results, we provide a few key insights about simulating Robot Links. A full treatment of Robot Link simulation will be provided in a future publication.

PyBullet does not natively support magnets, so we implemented them as external forces applied to the magnets inside the Robot Link connectors. To speed up the magnet computation, we only compute the magnet interaction between magnets within an empirically determined 14cm range, since magnet forces outside that range are negligible in a high-friction environment. Additionally, we used an occupancy grid to speed up the search for magnets within that range.

$$\vec{F}_{magnet_j} = \sum_{i \in A} K \frac{a_i * a_j}{|\vec{P_i} - \vec{P_j}|^3} (\vec{P_i} - \vec{P_j}) \quad (1)$$

The external force applied on $magnet_j$ is computed using (1), where A is the subset of magnets within 14cm range of $magnet_j$ and K is an empirically computed constant such that the attraction force of two simulated connectors equals the measured attraction force between two physical connectors. The magnet activation scalars $a_i, a_j \in [0,1]$ mimic the effect of the magnet retraction mechanism. Each magnet has We used random controller search, manual control, and hardcoded robot gates to explore the Robot Link dynamics in simulation.

A. Self-assembly

By crawling two non-parallel *links* to the point where their trajectories intersect, Robot Links can easily be assembled in plane. Forming a tetrahedron from a diamond-with-tail (a tetrahedron flat pattern) is challenging and requires out-of-plane motion. A diamond-with-tail is a low-energy formation, where all *links* are in contact with the ground plane. While a tetrahedron is a higher energy formation that requires three links to be lifted out of plane—gaining potential energy. To achieve this higher energy formation, the *links* must either be elevated and have energy potential or be moved to that state through servo motion or an external force. Our physical experiment environment allows the diamond-with-tail topology to move out of plane by crawling off a 30cm tall ledge that is followed by a cylindrical obstacle (shown in gray in Fig. 2-a.3). This setup enables the diamond-with-tail to fold-over on itself and become a tetrahedron—retaining some of its original potential energy in the tetrahedron structure.

In our experiment, we explored if a 3D structure could be formed from independent one-dimensional Robot Links. The experiment was conducted using six individual Robot Links placed on the first stage (Fig. 2-a.1) of our 1m by 4.3m experiment environment. First, the links attempt to form a triangle, and a three-pointed star topology. This step tests if single links can combine to form more capable Robot Link structures—both three-pointed stars and triangle topologies can move in two dimensions (2D), while individual links cannot. Next, moving to the second stage (Fig. 2-a.2), the triangle and the three-pointed star combine to form a diamond-with-tail shape, then fold into a tetrahedron.

B. Self-healing

The self-healing experiment is conducted on stage three and four without the cylindrical obstacle (visualized in Fig. 2 a.3 and a.4). In this experiment, a three-pointed star, a triangle, and a diamond-with-tail topology crawl off the 30cm ledge and attempt to recover from the resulting damage. For the purposes of this experiment, damage is defined as the destruction of the original robot topology, not physical damage to a Robot Link itself.

In this experiment, robots can experience two damage types: links or substructures that detach in part, and complete detachments, akin to losing a limb. The key distinction is that partial detachments don't risk losing the component, preserving a much higher chance for recovery.

IV. Results

The results of the *self-assembly* and *self-healing* experiments are shown in Fig. 2 and Fig. 3 respectively.

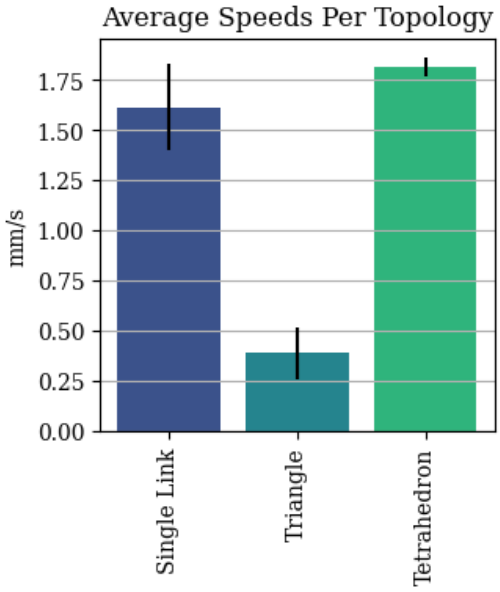


Figure 4. A graph showning the average speed of repeatedly crawling a single Robot Link, a triangle, and a tetrahedron down a 10-degree slope. The crawling gates were hardcoded based on empirical tests, and acts as a baseline to improve upon with learned controllers in the future.

A. Self-assembly

We found that three independent links can combine to form a triangle or a 3-pointed star (Fig. 2-b.1) configuration. Both of these transitions form fully controllable planar robots from Robot Links that, on their own, could only crawl in 1D. Next, we demonstrated that a triangle can connect to and integrate a 3-pointed star to form a diamond-with-tail (Fig. 2 b.1) shape. This transition showed how a robot integrates with another robot to improve its abilities: a diamond-with-tail can overcome 25mm tall thresholds, which neither a triangle nor a 3-pointed star can achieve (see Table I in the appendix). Finally, the diamond-with-tail successfully folded itself into a tetrahedron (Fig. 2-b.2) and thereby morphs from a planar robot into a 3D robot capable of overcoming a 25mm square-bar obstacle. The tetrahedron also is faster and more consistent in its speed than any previous topology (see Fig. 5).

These findings demonstrate that the Robot Link-based robots can “grow” in shape and self-improve by absorbing material from their environment or by absorbing other robots. See Table I in the appendix for an outline of the strengths and weaknesses of all Robot Link topologies covered in this work.

Authorized licensed use limited to: University of Southern California. Downloaded on November 11,2025 at 22:32:37 UTC from IEEE Xplore. Restrictions apply.

B. Self-healing

Fig. 3 shows the result of one successful damage recovery experiment for each tested topology: three-pointed star, triangle, and diamond-with-tail. Not all attempts were successful, and the challenges encountered are addressed below.

First, the impact entirely separated the three-pointed star (see Fig. 3-top). Then, the Robot Links slid and rolled uncontrolled (see Fig. 3-top t=81 and t=82) until they settled near each other after impact. The resultant settled state allowed the operator to re-form the three-pointed star topology. While this successfully demonstrates the ability to re-form the three-pointed star after complete separation, it also highlights its instability: each *link* of a three-pointed star is only position constrained on one end of the connector tip, and thus allows the *links* to flail while falling and during impact. In addition, the environment's topology influences the chances of reformation. Several attempts failed spectacularly, with links being flung down the ramp or rolling away, thereby making recovering the shape impossible within the bounds of the experiment. This mimics nature: a severed limb can only be reattached if retrieved.

Second, the triangle incurred a single disconnection upon impact, causing it to become a three-*link* chain (see Fig. 3-middle). A three-*link* chain is under-constrained and, therefore, harder to control than a triangle. However, shape recovery is significantly easier in this scenario than with a *link* that was separated and could get lost. A triangle is a fully constrained and, therefore, strong Robot Link configuration; it took several attempts until a disconnection occurred. In one failed attempt, the triangle lost an entire *link*, which, due to the sloped surface, rolled towards and connected at the vertex where the other two links were connected, forming a three-pointed star. In another failed attempt, a *link* disconnected, as shown in the successful experiment, but the operator didn't manage to re-form the triangle within the bounds of the filming setup and thus aborted the attempt.

Third, the diamond-with-tail suffered a separation of the three-pointed star from the triangle upon impact (see Fig. 3-bottom). From the *self-assembly* experiment, we know that a three-pointed star can combine itself with a triangle to form a diamond-with-tail. The triangle tip of the diamond-with-tail folds under itself while falling from the ledge at *t=68s*, breaking the connections between the three-pointed star and the triangle. Folding two connected Robot Links towards each other past the minimum attachment angle that the connectors will allow is the easiest way of breaking their connection since the Robot Link body acts as a lever while the edge of the connector acts as a pivot. In this experiment, the lever action resulting from the triangle folding underneath breaks both connections between the three-pointed star and the triangle almost simultaneously. The three-pointed star settles on top of the triangle at *t=70s* and then needs to move down from the triangle to connect to the triangle. Once the first connection was re-formed, the second could be attained. The case of a separated substructure is less severe than that of a separated single link since the substructures are controllable in 2D, while a single link is not.

We found that under-constrained structures, such as the three-pointed star and the diamond-with-tail, are more likely separate from a fall. The under-constraint parts can flail and build high angular momentum that leads to detachment if they're moving outside the attachment angle range of the Robot Link connector.

V. Limitations and Future Work

We present a truss modular robot designed to reconfigure its structure post-impact. Its magnetic connections enable it to detach and reattach without damage, allowing it to re-establish its original form. However, success isn't guaranteed; environmental factors, like a sloping surface, can cause the links to roll away and become irretrievable, leading to reassembly failures. In future work, we hope to characterize the uncertainties related to the environment and the capability of the Robot Links through randomized environment and control trials.

Our experiments utilized a human operator to emulate localization and control systems, a proxy for full autonomy. This method introduces potential bias, conflating human error with intrinsic factors. We're developing an autonomous platform equipped with machine vision to address this.

Given recent AI advances, we believe the bottleneck for autonomous robot organisms lies in the hardware and sensors, not the software. This also includes the current power capacity of only 40 minutes, limiting the physical experiments. We anticipate that further improvements in battery technology will lead to extended runtimes.

Robot Link structures come with pre-determined breaking points: their magnetic connections. This is both a feature and a flaw. While it protects individual Robot Links from damage during impact by breaking the magnetic bonds, it simultaneously is a limiting factor for the maximum size a Robot Link structure can achieve. The biggest physical Robot Link structure built to date is a manually assembled 16-*link* polyhedron. We observed a maximum of five connections formed at one point during our self-assembly experiments. Connecting more connectors at one point becomes increasingly difficult as the attachment space gets crowded.

Our goal is to form a self-sustaining robot ecology that can grow, self-repair, and thrive without human intervention aside from supplying more robot links. In future work, we will explore the robot organism's ability to shed and replace "dead" or broken Robot Links to remain operational.

VI. Conclusion

Our work showcases a truss-style MRR that self-assembles and self-improves. Thanks to Robot Links' ability to self-assemble, they can form robots that grow in size by integrating more links, making themselves faster or more agile, and recovering from damage within their lifetime. We showed different robots self-repair physically by reconnecting or reintegrating *links* after disconnections or separations.

Robot Links form reformable bonds instead of permanent bonds. Similar to how cells found in animals and humans can reform bonds[17]. The cell bond type—permanent or reformable—affects the developmental potential of an organism; similarly, it affects the formation and rearrangement capacity of the Robot Link platform. The capacity to grow

Authorized licensed use limited to: University of Southern California. Downloaded on November 11,2025 at 22:32:37 UTC from IEEE Xplore. Restrictions apply.

structures and self-heal are a direct result of this re-formable attachment style.

The work in this paper is a step towards a future in which truss robots can adapt and reshape instead of being pre-built for specific use cases. This work contributes to and tries to spark interest in the physical development aspect of developmental robotics research.

The growth trajectory of the world's robot population suggests that robots will outnumber humans. Who will build and repair all the robots? We believe that the burden of sustaining the robot population ultimately rests with robots. To address this problem, we work towards a self-sustaining robot ecology.

APPENDIX

The tetrahedron formation sequence shown in Fig. 2

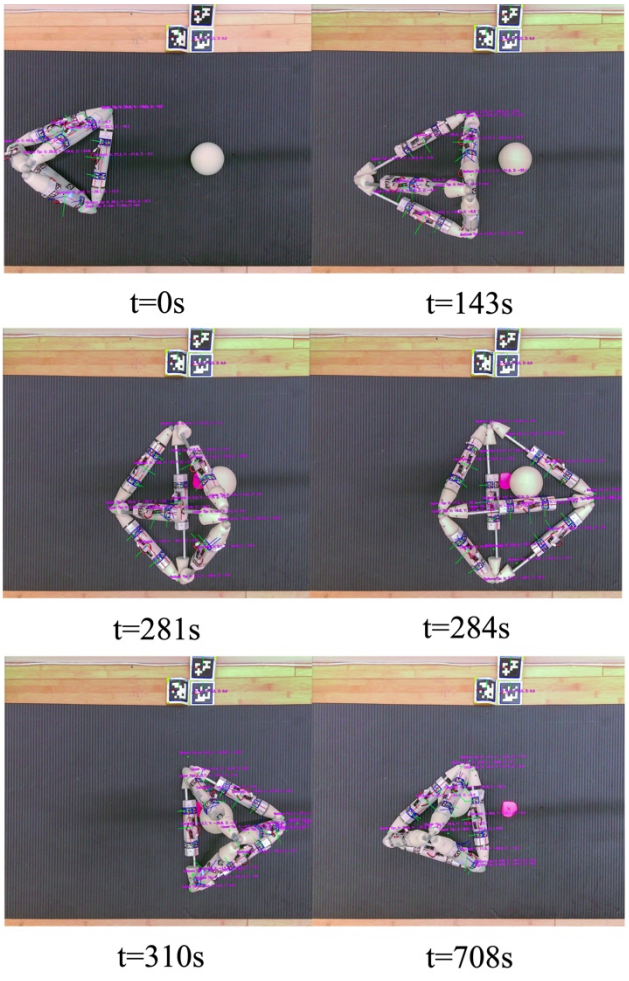


Figure 5. A frame sequences showing a tetrahedron made from Robot Links autonomously fetching a ball. It's pose was tracked using AprilTags placed on each Robot Link. The tetrahedron was programmed to topple once it reaches the target location and then crawl backwards.

demonstrates that Robot Links can form robots that manipulate their topology by exploiting the features of their environment; in Fig. 4, we illustrate how a tetrahedron made from Robot Links fetches a sphere placed at a known location by toppling onto it and then crawling with the sphere inside the tetrahedron. The frames shown in Fig. 4 are drawn from the top-down tracking camera of the "Long distance run" shown in the accompanying video. This experiment used a closed-loop script that tracked the tetrahedron's position using the AprilTag stickers applied to each link [18]. The tracking script uses the world tag at the top of each frame as the reference point for the tracking location. The payload is an FDM-printed plastic sphere 90mm in diameter with a weight of 93g. The experiment was implemented using a discrete set of commands: crawl, topple, and turn. The tetrahedron robot was programmed to crawl towards its target, adjusting direction with the turn command when necessary.

Table I shows seven Robot Link topologies and their strengths and weaknesses to highlight their differences. The structures formed in the *self-assembly* experiment are incrementally improving compared to their previous configurations as they "grow," their improvements are listed in the table.

TABLE I. BASIC TOPOLOGY OVERVIEW

Topology	**Attributes**		
	Nr. Links	***Strength***	***Weakness***
Single Link	1	Stable topology	1D movement
2-Link chain	2	2D movement	Inconsistent control behavior Unstable topology Unable to scale thresholds
3-Link chain	3	2D movement	Inconsistent control behavior Unstable topology Unable to scale thresholds
3-pointed star	3	Coordinated 2D movement	Unstable topology Unable to scale thresholds
Triangle	3	Coordinated 2D movement Stable topology	Slow Unable to scale 25mm thresholds
Diamond-with-tail	6	Can scale 25mm thresholds Coordinated 2D movement Able to form tetrahedron	Slow Unable to overcome 25mm ledge
Tetrahedron	6	Stable 3D motion: crawling and toppling Overcomes 3D 25mm ledge	May collapse on impact or when moved outside its stable configuration space

ACKNOWLEDGMENT

Thanks to Rui Chu for contributing to the simulation. Thanks to Claudio Vicentelli for inspiring us with GEOMAG.

REFERENCES

[1] T. Mikolajczyk *et al.*, "Recent Advances in Bipedal Walking Robots: Review of Gait, Drive, Sensors and

Authorized licensed use limited to: University of Southern California. Downloaded on November 11,2025 at 22:32:37 UTC from IEEE Xplore. Restrictions apply.

Control Systems," *Sensors*, vol. 22, no. 12, 2022, doi: 10.3390/s22124440.

[2] A. Fukuhara, M. Gunji, and Y. Masuda, "Comparative anatomy of quadruped robots and animals: a review," *Advanced Robotics*, vol. 36, no. 13, 2022, doi: 10.1080/01691864.2022.2086018.

[3] L. Von Bertalanffy, "The Theory of Open Systems in Physics and Biology," *Science (1979)*, vol. 111, no. 2872, pp. 23–29, 1950, Accessed: Nov. 21, 2022. [Online]. Available: http://www.jstor.org/stable/1676073

[4] J. Seo, J. Paik, and M. Yim, "Modular Reconfigurable Robotics," *https://doi.org/10.1146/annurev-control-053018-023834*, vol. 2, pp. 63–88, May 2019, doi: 10.1146/ANNUREV-CONTROL-053018-023834.

[5] A. Lyder, R. F. M. Garcia, and K. Stoy, "Mechanical design of Odin, an extendable heterogeneous deformable modular robot," in *2008 IEEE/RSJ International Conference on Intelligent Robots and Systems, IROS*, IEEE, Sep. 2008, pp. 883–888. doi: 10.1109/IROS.2008.4650888.

[6] C. H. Yu, K. Haller, D. Ingber, and R. Nagpal, "Morpho: A self-deformable modular robot inspired by cellular structure," in *2008 IEEE/RSJ International Conference on Intelligent Robots and Systems, IROS*, IEEE, Sep. 2008, pp. 3571–3578. doi: 10.1109/IROS.2008.4651130.

[7] A. Spinos, D. Carroll, T. Kientz, and M. Yim, "Variable topology truss: Design and analysis," *IEEE International Conference on Intelligent Robots and Systems*, vol. 2017-September, pp. 2717–2722, Dec. 2017, doi: 10.1109/IROS.2017.8206098.

[8] E. Park, J. Bae, S. Park, J. Kim, M. Yim, and T. W. Seo, "Reconfiguration solution of a variable topology truss: Design and experiment," *IEEE Robot Autom Lett*, vol. 5, no. 2, pp. 1939–1945, Apr. 2020, doi: 10.1109/LRA.2020.2970618.

[9] M. Yim, D. G. Duff, and K. D. Roufas, "PolyBot: a modular reconfigurable robot," in *Proceedings 2000 ICRA. Millennium Conference. IEEE International Conference on Robotics and Automation. Symposia Proceedings (Cat. No.00CH37065)*, IEEE, 2000, pp. 514–520. doi: 10.1109/ROBOT.2000.844106.

[10] S. Murata, E. Yoshida, A. Kamimura, H. Kurokawa, K. Tomita, and S. Kokaji, "M-TRAN: Self-reconfigurable modular robotic system," *IEEE/ASME Transactions on Mechatronics*, vol. 7, no. 4, pp. 431–441, Dec. 2002, doi: 10.1109/TMECH.2002.806220.

[11] A. Spröwitz, R. Moeckel, M. Vespignani, S. Bonardi, and A. J. Ijspeert, "Roombots: A hardware perspective on 3D self-reconfiguration and locomotion with a homogeneous modular robot," *Rob Auton Syst*, vol. 62, no. 7, pp. 1016–1033, Jul. 2014, doi: 10.1016/j.robot.2013.08.011.

[12] J. Baca, S. G. M. Hossain, P. Dasgupta, C. A. Nelson, and A. Dutta, "ModRED: Hardware design and reconfiguration planning for a high dexterity modular self-reconfigurable robot for extra-terrestrial exploration," *Rob Auton Syst*, vol. 62, no. 7, pp. 1002–1015, 2014, doi: 10.1016/j.robot.2013.08.008.

[13] T. M. Roehr, F. Cordes, and F. Kirchner, "Reconfigurable integrated multirobot exploration system (RIMRES): Heterogeneous modular reconfigurable robots for space exploration," *J Field Robot*, vol. 31, no. 1, pp. 3–34, 2014, doi: 10.1002/rob.21477.

[14] Y. Tu, G. Liang, and T. L. Lam, "FreeSN: A Freeform Strut-node Structured Modular Self-reconfigurable Robot - Design and Implementation," *Proc IEEE Int Conf Robot Autom*, pp. 4239–4245, 2022, doi: 10.1109/ICRA46639.2022.9811583.

[15] G. Liang, H. Luo, M. Li, H. Qian, and T. L. Lam, "FreeBOT: A Freeform Modular Self-reconfigurable Robot with Arbitrary Connection Point-Design and Implementation," *2020 IEEE/RSJ International Conference on Intelligent Robots and Systems (IROS)*, no. October, pp. 6506–6513, 2020.

[16] E. Coumans and Y. Bai, "PyBullet, a Python module for physics simulation for games, robotics and machine learning."

[17] T. C. Day *et al.*, "Varied solutions to multicellularity: The biophysical and evolutionary consequences of diverse intercellular bonds," *Biophys Rev*, vol. 3, no. 2, p. 021305, Jun. 2022, doi: 10.1063/5.0080845.

[18] E. Olson, "AprilTag: A robust and flexible visual fiducial system," *Proc IEEE Int Conf Robot Autom*, pp. 3400–3407, 2011, doi: 10.1109/ICRA.2011.5979561.

Authorized licensed use limited to: University of Southern California. Downloaded on November 11,2025 at 22:32:37 UTC from IEEE Xplore. Restrictions apply.